JIEET (Journal of Information Engineering and Educational Technology)

Volume 9, Number 2, 2025 pp. 129-140
E-ISSN : 2549-869X
Open Access: https://journal.unesa.ac.id/index.php/jieet

Early Detection of Melanoma Using an Android-Based Hybrid FCM-CNN Algorithm

Alda Ellsa Faradilla[1*], Wiyli Yustanti[2]
[1,2] Department of Informatics, Universitas Negeri Surabaya, Surabaya, Indonesia

Corresponding author: wiyly@unesa.ac.id

ARTICLE INFO

Article history:
Submitted 17-05-2025
Accepted 5-12-2025
Available online 6-12-2025

Keywords:
Melanoma, Early Detection, Android, Fuzzy C-Means (FCM), Convolutional Neural Network (CNN).

DOI:
https://doi.org/10.26740/jieet.v9n2.p129-140

ABSTRACT

According to the Global Cancer Observatory, the lowest melanoma cases occurred in the Asian population at around 25% of the 100,000 population in 2018. Melanoma is a malignancy of melanocytes, the melanin (pigment) producing cells in the basal layer of the epidermis. This research aims to increase the likelihood of cure and decrease the mortality rate from melanoma by implementing an Android-based hybrid Fuzzy C-Means (FCM) and Convolutional Neural Network (CNN) algorithm using the 2017 ISIC dataset. This algorithm leverages FCM's segmentation strengths, including creating more uniform regions, minimizing blob dispersion, reducing noise, and lowering noise sensitivity. It also employs CNN for classification, automatically extracting features from training data, reducing reliance on diverse base features, and potentially enhancing training quality. The application was developed using Kotlin, with the CRISP-DM methodology for data analysis, including business understanding, data understanding, data preparation, modelling, evaluation, and deployment using Rapid Application Development (RAD). Model evaluation is performed using K-Fold Cross-Validation, and application testing is conducted using Black-Box Testing. The results show that the FCM-CNN hybrid model achieves the best performance on an 80:20 dataset split, with 50 epochs, a batch size of 16, the Adam optimiser, and K-Fold 10, achieving 99.42% accuracy. The results of the analysis test for the detection application, conducted using a remote detector camera on a Samsung A23 smartphone, showed an average accuracy of 78.33%. This research is expected to contribute to the development of medical technology to identify melanoma early.

INTRODUCTION

According to the Global Cancer Observatory, the lowest incidence of melanoma occurs in Asian populations, at around 25 per 100,000 people in 2018 (Rinonce et al., 2022). Melanoma is a cancer that arises from melanocytes, cells that produce melanin (pigment), in the basal layer of the epidermis. The often-undetected presence of melanoma is one of the reasons for the high mortality rate from this skin cancer. Lack of awareness and knowledge about the early symptoms of melanoma means that many new cases go undetected. To diagnose skin cancers such as

melanoma, a biopsy is usually performed, in which a sample of skin tissue is removed and examined under a microscope.

Therefore, there is a need for the application of melanoma early detection technology that is more accessible and affordable to increase the chances of recovery and reduce mortality rates from melanoma. This study utilises the 2017 ISIC dataset to apply this technology in the medical world. Several studies have been conducted to prove the accuracy of the algorithms used in other studies. For example, one study using a Convolutional Neural Network (CNN) achieved 82% accuracy. (Yilmaz et al., 2021). Another study used the Mask R-CNN algorithm to implement the technology on the ISIC 2017 dataset, achieving 90% accuracy. (Jojoa Acosta et al., 2021). Another study using the Mask R-CNN algorithm produced a melanoma research accuracy of 90.85% (Goyal et al., 2020). And research using the Deep Convolutional Generative Adversarial Networks (DCGANs) algorithm produced an accuracy of 81.60% (Bisla et al., 2019).

Although algorithms such as CNNs, Mask R-CNN, and DCGANs have achieved high accuracy in studies using the ISIC 2017 dataset, each still has weaknesses that can affect its performance. CNN, when predicting images with similar shapes and containing many objects, the error rate will increase, so the possibility of errors in predicting image results becomes greater (Reza Fahcruroji et al., 2024). Mask R-CNN requires high computational resources. (Setyaningsih & Edy, 2022). DCGANs suffer from instability during training due to convergence issues, leading to inconsistent results given their generative nature. (Jenkins & Roy, 2024). Therefore, a hybrid algorithm is needed that can combine the advantages of several algorithms to overcome these weaknesses. One approach is the FCM-CNN algorithm, which combines the Fuzzy C-Means (FCM) algorithm with Convolutional Neural Networks (CNN).

The FCM-CNN hybrid algorithm has been proven effective in research published in the journal "Enhanced Automatic Classification of Brain Tumours with FCM and Convolution Neural Network", with an accuracy of 91% (Rao et al., 2020). This algorithm leverages the segmentation advantages of Fuzzy C-Means, including producing more homogeneous areas than other methods, reducing the spread of blobs, eliminating noise spots, and minimizing sensitivity to noise. This algorithm also utilises a CNN in the classification process, which automatically extracts features from the training data, eliminating reliance on specific features and potentially improving training quality.

The Android platform offers simple access and excellent flexibility, making it an ideal choice for Artificial Intelligence (AI)-based applications. This research is expected to make a significant contribution to health, particularly oncology, as well as to information technology through the development of innovative mobile applications. In addition, this research provides new insights into the application of artificial intelligence, especially FCM-CNN.

METHOD

This study uses a quantitative approach, with the CRISP-DM (Cross Industry Standard Process for Data Mining) framework as the basis for designing and implementing algorithms for melanoma early detection applications. This framework consists of six main stages, namely

business understanding, data understanding, data preparation, modelling, evaluation, and implementation, which help researchers organise their workflow systematically and comprehensively. The research approach is applied, with a focus on developing machine learning-based applications. Data was collected through an online, open-source skin image dataset. Data analysis was performed by preprocessing (e.g., CLAHE and Monte Carlo Denoising), segmenting with Fuzzy C-Means, extracting features using GLCM, and classifying with a CNN. The CRISP-DM framework has proven effective as a guide in various case studies, including the development of machine learning-based applications. This has been proven in research on visitor review classification (Singgalen, 2023) and the problem of clustering fire-prone areas (Dhewayani et al., 2022).

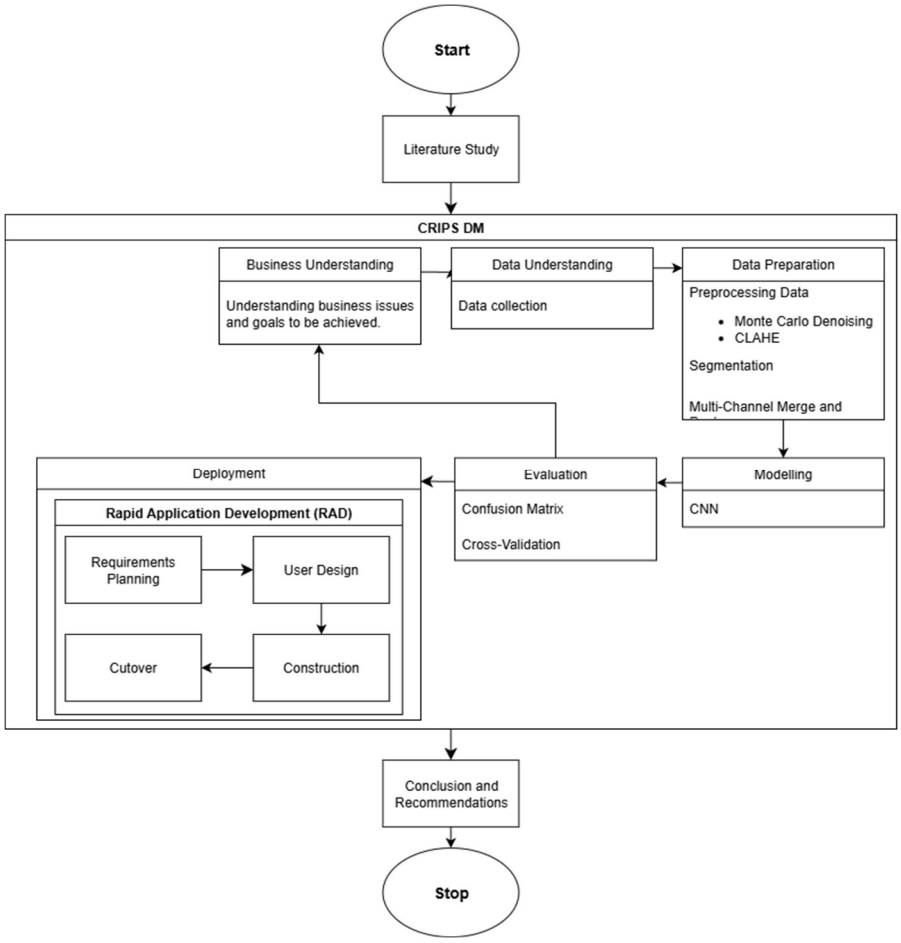

Figure 1. Framework CRISP-DM.

RESULTS

1. Result of Data Pre-processing

The initial step in image processing is labelling each image according to its originating folder: healthy skin (label 0), melanoma (label 1), or non-melanoma (label 2). These labels are used as class markers during model training and testing. All images were read from three separate

folders by class, then uniformly resized to 100×100 pixels to be compatible with the Convolutional Neural Network (CNN) architecture. After size normalisation, image quality was improved through the Monte Carlo Denoising method to reduce noise that could interfere with feature extraction (Huo & Yoon, 2021). This process results in a smoother, more natural pixel distribution by removing anomalous values that reflect visual noise. Next, contrast enhancement is performed using the Contrast Limited Adaptive Histogram Equalisation (CLAHE) method via the apply_clahe function to achieve more even lighting and improve the sharpness of image details (Momeni Pour et al., 2020).

```
Matriks piksel sebelum denoising
Channel 0:
[[ 3  3  3  3  3  3  3  3  0  0]
 [ 3  3  3  3  3  3  3  3  5  3]
 [ 3  3  3  3  3  3  3  3 10  8]
 [ 3  3  3  3  3  3  3  3  7  6]
 [ 3  3  3  3  3  3  3  3  0  0]
 [ 3  3  3  3  3  3  3  3  0  0]
 [ 3  3  3  3  3  3  3  3  1  4]
 [ 3  3  3  3  3  3  3  3  8 10]
 [ 8  5  1  0  0  1  5  8 11  6]
 [ 8  5  1  0  0  1  5  8  9  4]]
```

```
Matriks piksel setelah denoising
Channel 0:
[[ 2  0  2  4  4  2  2  0  0  0]
 [ 6  3  2  4  1  5  6  0  6  3]
 [ 2  5  0  3  6  1  3  2  8  6]
 [ 0  0  5  1  6  2  5  3  4  6]
 [ 0  7  4  0  3  3  3  4  0  2]
 [ 6  0  1  3  0  1  1  0  0  0]
 [ 8  3  4  0  4  0  1  2  1  5]
 [ 4  0  3  2  4  6  4  3 11  9]
 [ 6  5  0  0  0  2  5 13 12  9]
 [ 9  4  4  0  0  0  6  7  7  1]]
```

Figure 2. Monte Carlo Denoising Pixel Matrix.

Before denoising, the top pixels appear relatively uniform, with almost all values set to 3. However, there are some anomalies or noise, such as spikes in the bottom-right corner (e.g., values 10 and 11), indicating interference or unnatural sharp edges. After denoising, the pixel values become more varied but smoother, no longer dominated by the number 3, and exhibit a more natural transition between pixels.

```
Matriks L channel sebelum CLAHE
[[ 2  2  3  1  1  0  2  1  1  1]
 [ 1  1  2  1  3  2  1  1  3  6]
 [ 1  2  2  2  2  0  1  2  6  7]
 [ 2  2  2  1  1  1  2  1  6  5]
 [ 2  2  2  1  1  1  2  2  0  1]
 [ 1  2  2  1  2  2  0  2  1  0]
 [ 2  0  2  1  1  1  1  5  0  1]
 [ 2  2  2  1  1  0  1  2  5  7]
 [ 6  3  0  0  1  1  2  2 11  5]
 [ 5  5  1  0  1  0  2  7  6  0]]
```

```
Matriks piksel setelah CLAHE
Channel 0:
[[13 13 16  8 13  4 13 13  6  6]
 [ 6 11 10 11 16 10 11 11 10 19]
 [ 6 10 13  8 13  9  8 13 24 21]
 [10 10 15 13 13  6 15  8 19 18]
 [16  8 16  8  8  6 15 10  9  6]
 [11 10 15  8 10 15  9  8  6  6]
 [16  9 16 13 13 11  6 19  4 13]
 [10 10 10  6 11  9 13 10 19 25]
 [19 16  4  6  6  6 13 15 30 17]
 [21 15  6  4  6  6 13 21 20  4]]
```

Figure 3. CLAHE Pixel Matrix.

In the initial condition, the pixel values in the area have a narrow range, ranging from 0 to 7. After applying the CLAHE process shown in the second image, the distribution of pixel values changes significantly. The previously small values are now more widely distributed, with numbers reaching up to 25. This means that the local contrast within the area has been enhanced.

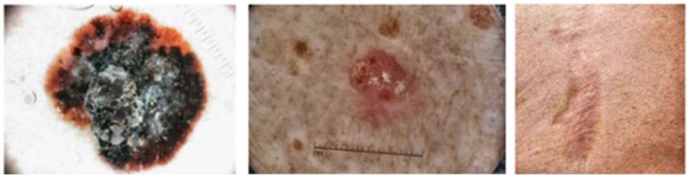

Figure 4. Pre-Processing Result.

2. Result of Segmentation

After data preprocessing, segmentation is performed using the Fuzzy C-Means (FCM) algorithm. After the image is segmented, the extract_glcm_features function extracts texture features using the Grey-Level Co-Occurrence Matrix (GLCM) method, which helps detect texture patterns by providing statistical information about grey-level co-occurrences in an image. Melanomas are classified into three types based on thickness: thin (<0.76 mm), intermediate (0.76-1.5 mm), and thick (>1.5 mm). Thin melanomas generally have a smooth, homogeneous texture, characterised by high homogeneity and energy values and low contrast, reflecting the still uniform tissue. In intermediate melanoma, texture irregularities begin to appear as cancer cells penetrate the dermis, leading to increased contrast and correlation values. Meanwhile, thick melanoma shows a rough, irregular texture, with high contrast, low homogeneity, and decreased correlation, reflecting greater tissue invasion and complexity. (Patil & Bellary, 2022).

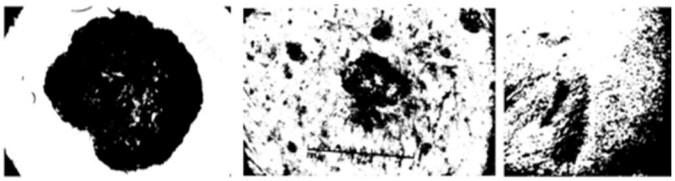

Figure 5. Segmentation Result.

3. Hybrid FCM-CNN

At this stage, the original image is combined with the FCM segmentation result mask as an additional channel, so the CNN receives four input channels: 3 RGB channels and 1 FCM segmentation channel. CNN will learn the combination of the original image and the segmentation results, so FCM provides additional information such as colour, texture, and object shape. After all images undergo data preprocessing and segmentation and are assigned to the specified folder, the data is converted to an array so the CNN layer can capture information from the features generated.

4. Modelling

Table 1. Amount of Training and Testing Data.

Data	Proportion of 30% Test	Proportion of 20% Test	Proportion of 10% Test
Training Data	840	960	1080
Testing Data	361	241	121

Table 1 shows the proportion of the melanoma dataset available on Kaggle, typically images labelled to support research on developing melanoma detection models. This dataset for melanoma detection was obtained from John C's ISIC-2017 dataset, which contains images of two types of skin cancer: melanoma and seborrheic keratosis (nevus).

Table 2. Model Summary.

Layer	Output Shape	Parameter
conv2d_12 (Conv2D)	(None, 100, 100, 32)	1,184
max_pooling2d_12 (MaxPooling2D)	(None, 50, 50, 32)	0
conv2d_13 (Conv2D)	(None, 50, 50, 64)	18,496
max_pooling2d_13 (MaxPooling2D)	(None, 25, 25, 64)	0
conv2d_14 (Conv2D)	(None, 25, 25, 128)	73,856
max_pooling2d_14 (MaxPooling2D)	(None, 12, 12, 128)	0
flatten_4 (Flatten)	(None, 18432)	0
dense_7 (Dense)	(None, 128)	2,359,424
Dropout_4 (Dropout)	(None, 128)	0
dense_8 (Dense)	(None, 3)	387

Table 2 model summary shows that the Convolutional Neural Network (CNN) architecture used in this study has a total of 2,453,059 trainable parameters. The CNN layer consists of three convolutional layers, each followed by a pooling layer, which gradually reduce the data dimension from 100x100x32 to 12x12x128 by extracting important features from the input image. The Flatten layer then converts the data into a 1D vector of size 18,432, which is further processed by two Dense layers. The first Dense layer has 128 units, followed by a Dropout layer to reduce overfitting. The last layer is a Dense layer with three units for class classification. (Islam et al., 2020).

Table 3. Hyperparameter Tuning Test.

Parameter	Value
Batch Size	16, 32
Epoch	50, 100

5. Evaluation

1) K-fold 3

Table 4. K-Fold 3 Model Evaluation Results.

Scale of Dataset Division	Batch Size	Epoch	Testing Accuracy	Training Accuracy
70:30	16	50	0.9593	0.9963
70:30	16	100	0.9709	0.9979
70:30	32	50	0.9750	0.9992
70:30	32	100	0.9501	0.9979

80:20	16	50	0.9884	0.9950
80:20	16	100	0.9734	0.9988
80:20	32	50	0.9742	1.0000
80:20	32	100	0.9717	1.0000
90:10	16	50	0.9617	0.9967
90:10	16	100	0.9626	0.9996
90:10	32	50	0.9667	0.9983
90:10	32	100	0.9601	0.9992

2) K-Fold 5

Table 5. K-Fold 5 Model Evaluation Results.

Scale of Dataset Division	Batch Size	Epoch	Testing Accuracy	Training Accuracy
70:30	16	50	0.9792	0.9988
70:30	16	100	0.9851	0.9992
70:30	32	50	0.9809	0.9996
70:30	32	100	0.9817	0.9994
80:20	16	50	0.9801	0.9983
80:20	16	100	0.9867	0.9996
80:20	32	50	0.9909	0.9977
80:20	32	100	0.9817	0.9990
90:10	16	50	0.9859	0.9923
90:10	16	100	0.9817	0.9996
90:10	32	50	0.9842	0.9975
90:10	32	100	0.9734	0.9967

3) K-Fold 10

Table 6. K-Fold 10 Model Evaluation Results.

Scale of Dataset Division	Batch Size	Epoch	Testing Accuracy	Training Accuracy
70:30	16	50	0.9767	0.9960
70:30	16	100	0.9867	0.9989
70:30	32	50	0.9934	0.9983
70:30	32	100	0.9909	0.9983
80:20	16	50	0.9942	0.9946
80:20	16	100	0.9934	0.9944
80:20	32	50	0.9917	0.9971
80:20	32	100	0.9926	0.9995
90:10	16	50	0.9892	0.9980
90:10	16	100	0.9925	0.9992
90:10	32	50	0.9925	0.9975
90:10	32	100	0.9909	0.9981

In the Table above, the highest and optimal accuracy results from all experiments are obtained with epoch 50, batch size 16, Adam optimiser, and an 80% training, 20% testing dataset split, with k-fold 10. The best results were testing accuracy of 0.9942 and training accuracy of 0.9946.

6. Deployment

This research adopts the Rapid Application Development (RAD) method as its primary approach to software development. This method focuses on deeply understanding user needs by actively involving users during the development cycle. After the model is trained and saved in HDF5 (.h5) format, the next step is to convert it to TensorFlow Lite (.tflite) format for integration into the Android application.

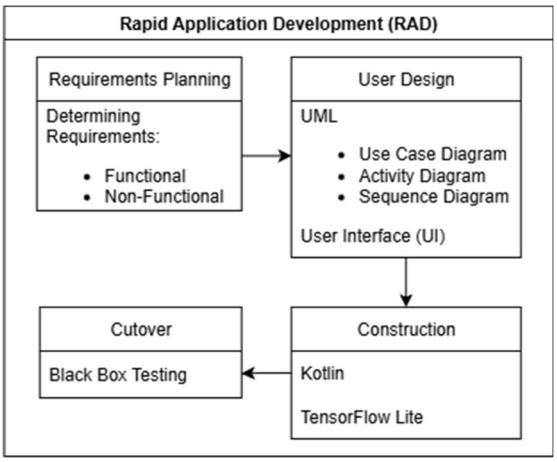

Figure 6. Rapid Application Development (RAD) Method.

7. Result of Application

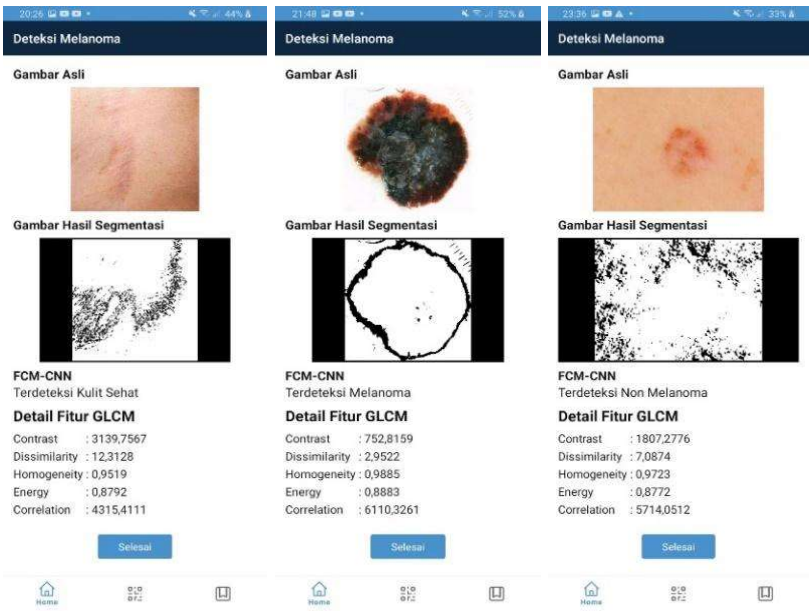

Figure 7. Melanoma Early Detection Application.

Table 7. List of Smartphones.

No	Smartphone	Camera Resolution
1	Samsung A30s	25 mp
2	Samsung A23	50 mp
3	Samsung A35	50 mp

Table 8. Black Box Testing Results.

Test Scenarios	Expected Results	Results		
		1	2	3
Opening the App	Displays the home page.	✓	✓	✓
Clicking the home menu	Displays the home page.	✓	✓	✓
Clicking the "Select Image" button	Displays a gallery for uploading images.	✓	✓	✓
Clicking the "Detection" button	Displays the detection results.	✓	✓	✓
Clicking the scan menu	Displays the camera detector in real time.	✓	✓	✓
Clicking the "Finish" button	Saves the detection results in .pdf format to the smartphone storage.	✓	✓	✓
Clicking the instructions menu	Displays the instructions page.	✓	✓	✓

Analysis of detection results is performed to further test the detection features of melanoma applications under various conditions and at different distances from the skin.

1) Import Gallery

   From the analysis of test results for the application using imported images, the highest average accuracy is obtained with a Samsung A23 smartphone, with a total accuracy of 0.7500. With a healthy skin detection accuracy of 0.8500, melanoma of 0.7500, and non-melanoma of 0.6500. The quality of the input images influences the accuracy of the results, the unoptimized segmentation processing, and the smartphone software.

2) Close-range Detection Camera

   From the analysis of the application using a close-range camera detector, the highest average accuracy is achieved with a Samsung A23 smartphone, with a total accuracy of 0.7166. With a healthy skin detection accuracy of 1.0000, melanoma of 0.6500, and non-melanoma of 0.5000. Image capture conditions influence this accuracy; the segmentation process is not optimal, and smartphone software.

3) Long-range Detection Camera

From the analysis of the application using a long-range camera detector, the highest average total accuracy is achieved with a Samsung A23 smartphone, at 0.7833. With a healthy skin detection accuracy of 1.0000, melanoma of 0.8000, and non-melanoma of 0.5500. Image capture conditions, suboptimal segmentation processes, and smartphone software influence this accuracy.

DISCUSSION

The results of the study show that combining FCM and CNN algorithms can improve the system's ability to detect melanoma, as FCM segmentation yields a more homogeneous lesion area with minimal noise, thereby enabling the CNN to extract visual features more effectively. These findings align with previous research on medical images, which also reported improved performance with the FCM-CNN hybrid approach. However, in this study, the achieved accuracy was higher than that of single algorithms such as CNNs, Mask R-CNNs, and DCGANs on the ISIC 2017 dataset. Although the model performed very well in a controlled environment, its implementation in an Android application showed a decrease in accuracy in real-world conditions, due to variations in camera quality, lighting, and FCM segmentation that were not yet optimal on mobile devices. This performance difference shows that, although the model is effective during training, integrating it into mobile devices requires further optimisation to ensure more stable, consistent detection results across different conditions. These findings emphasise the importance of improving segmentation and standardising input quality in the development of future Android-based melanoma detection systems.

CONCLUSION

Based on research on the melanoma detection system using the Android-based FCM-CNN algorithm, it can be concluded that the FCM-CNN hybrid model developed and applied achieves an optimal accuracy of 99%. 42% of the overall experiment was conducted using epoch 50, batch size 16, the Adam optimiser, and an 80% training, 20% testing split across 10 folds. This result is better than the evaluation results of other studies using the 2017 ISIC dataset using CNN at 82% (Yilmaz et al., 2021), Mask R-CNN at 90% (Jojoa Acosta et al., 2021) and 90.85% (Goyal et al., 2020), and DCGANs at 81.60% (Bisla et al., 2019). This shows that the hybrid model achieves high accuracy in recognising melanoma.

An Android-based melanoma detection application, developed in Kotlin and integrating TensorFlow Lite, can detect melanoma by combining the FCM algorithm for image segmentation and a CNN for visual feature extraction. The results of the analysis test for the most optimal melanoma detection application were as follows: healthy skin, 1.0000; melanoma, 0.8000; and non-melanoma, 0.5500. Image capture conditions influence these results; the FCM-based segmentation process in Android is not optimal, and the smartphone software used is not optimal either.

REFERENCES

Bisla, D., Choromanska, A., Berman, R. S., Stein, J. A., Polsky, D., & Perelman, R. O. (2019). *Towards Automated Melanoma Detection with Deep Learning: Data Purification and Augmentation*. https://github.com/

Dhewayani, F. N., Amelia, D., Alifah, D. N., Sari, B. N., Jajuli, M., HSRonggo Waluyo, J., Telukjambe Timur, K., Karawang, K., & Barat, J. (2022). Implementasi K-Means Clustering untuk Pengelompokkan Daerah Rawan Bencana Kebakaran Menggunakan Model CRISP-DM. *Jurnal Teknologi Dan Informasi*. https://doi.org/10.34010/jati.v12i1

Goyal, M., Oakley, A., Bansal, P., Dancey, D., & Yap, M. H. (2020). Skin Lesion Segmentation in Dermoscopic Images with Ensemble Deep Learning Methods. *IEEE Access*, *8*, 4171–4181. https://doi.org/10.1109/ACCESS.2019.2960504

Huo, Y., & Yoon, S. Eui. (2021). A survey on deep learning-based Monte Carlo denoising. In *Computational Visual Media* (Vol. 7, Issue 2, pp. 169–185). Tsinghua University. https://doi.org/10.1007/s41095-021-0209-9

Islam, M. Z., Islam, M. M., & Asraf, A. (2020). A combined deep CNN-LSTM network for the detection of novel coronavirus (COVID-19) using X-ray images. *Informatics in Medicine Unlocked*, *20*. https://doi.org/10.1016/j.imu.2020.100412

Jenkins, J., & Roy, K. (2024). Exploring deep convolutional generative adversarial networks (DCGAN) in biometric systems: a survey study. In *Discover Artificial Intelligence* (Vol. 4, Issue 1). Springer Nature. https://doi.org/10.1007/s44163-024-00138-z

Jojoa Acosta, M. F., Caballero Tovar, L. Y., García-Zapirain, M. B., & Percybrooks, W. S. (2021). Melanoma diagnosis using deep learning techniques on dermatoscopic images. *BMC Medical Imaging*, *21*(1). https://doi.org/10.1186/s12880-020-00534-8

Momeni Pour, A., Seyedarabi, H., Abbasi Jahromi, S. H., & Javadzadeh, A. (2020). Automatic detection and monitoring of diabetic retinopathy using efficient convolutional neural networks and contrast-limited adaptive histogram equalization. *IEEE Access*, *8*, 136668–136673. https://doi.org/10.1109/ACCESS.2020.3005044

Patil, R., & Bellary, S. (2022). Machine learning approach in melanoma cancer stage detection. *Journal of King Saud University - Computer and Information Sciences*, *34*(6), 3285–3293. https://doi.org/10.1016/j.jksuci.2020.09.002

Rao, L. J., Challa, R., Sudarsa, D., Naresh, C., & Basha, C. Z. (2020). Enhanced automatic classification of brain tumours with FCM and convolution neural network. *Proceedings of the 3rd International Conference on Smart Systems and Inventive Technology, ICSSIT 2020*, 1233–1237. https://doi.org/10.1109/ICSSIT48917.2020.9214199

Reza Fahcruroji, A., Yunita Wijaya, M., Fauziah, I., Sains dan Teknologi, F., Syarif Hidayatullah Jakarta Jl Ir Juanda No, U. H., Ciputat Tim, K., & Tangerang Selatan, K. (2024). IMPLEMENTASI ALGORITMA CNN MOBILENET UNTUK KLASIFIKASI GAMBAR SAMPAH DI BANK SAMPAH. *PROSISKO: Jurnal Pengembangan Riset Dan Observasi Sistem Komputer*, 45–51.

Rinonce, H. T., Sastri, D. J., Trisnawati, F., Kameswari, B., Ferronika, P., & Irianiwati. (2022). The frequency and clinicopathological significance of NRAS mutations in primary cutaneous nodular melanoma in Indonesia. *Cancer Reports*, *5*(1). https://doi.org/10.1002/cnr2.1454

Setyaningsih, E. R., & Edy, M. S. (2022). YOLOv4 dan Mask R-CNN Untuk Deteksi Kerusakan Pada Karung Komoditi. *Teknika*, *11*(1), 45–52. https://doi.org/10.34148/teknika.v11i1.419

Singgalen, Y. A. (2023). Penerapan Metode CRISP-DM untuk Optimalisasi Strategi Pemasaran STP (Segmenting, Targeting, Positioning) Layanan Akomodasi Hotel, Homestay, dan Resort. *JURNAL MEDIA INFORMATIKA BUDIDARMA*, *7*(4), 1980. https://doi.org/10.30865/mib.v7i4.6896

Yilmaz, A., Kalebasi, M., Samoylenko, Y., Guvenilir, M. E., & Uvet, H. (2021). *Benchmarking of Lightweight Deep Learning Architectures for Skin Cancer Classification using ISIC 2017 Dataset*. http://arxiv.org/abs/2110.12270